PLB2Tau mice are impaired in novel and temporal object recognition and show corresponding traits in brain MRI

Jacques Micheau, Gwenaelle Catheline, Elodie Barse, Bassem Hiba, Anne Marcilhac, Michèle Allard, Bettina Platt, Gernot Riedel

Brain Research Bulletin 220 (2025) 111161

Contents lists available at ScienceDirect

Brain Research Bulletin

journal homepage: www.elsevier.com/locate/brainresbull

Research report

$PLB2_{Tau}$ mice are impaired in novel and temporal object recognition and show corresponding traits in brain MRI

Jacques Micheau [a,b,c], Gwenaelle Catheline [a,b], Elodie Barse [b], Bassem Hiba [d], Anne Marcilhac [e], Michèle Allard [b], Bettina Platt [f,g], Gernot Riedel [f,g,*]

[a] University of Bordeaux, UMR CNRS 5287, EPHE-PSL, 176 rue Léo Saignat, Bordeaux Cedex 33076, France
[b] Aquitaine Institute for Cognitive and Integrative Neurosciences, UMR CNRS 5287, EPHE-PSL, 176 rue Léo Saignat, Bordeaux Cedex 33076, France
[c] Present address: Neurocentre Magendie, University of Bordeaux, INSERM U862, 146, rue Léo Saignat, Bordeaux cedex 33076, France
[d] Institute of Cognitive Sciences Marc Jeannerod, University of Lyon 1, UMR CNRS 5229, Bron 69500, France
[e] MMDN, University of Montpellier 2, INSERM U1198 – EPHE-PSL University, Montpellier 34095, France
[f] Institute of Medical Sciences, University of Aberdeen, Foresterhill, Aberdeen AB25 2ZD, UK
[g] School of Medicine, Medical Sciences & Nutrition, University of Aberdeen, Foresterhill, Aberdeen AB25 2ZD, UK

ARTICLE INFO

Keywords:
HTau KI mice
Age profile
Object recognition
Episodic-like memory
MRI
ROIs volume
DTI
Fronto-temporal dementia

ABSTRACT

Recent clinical trials targeting tau protein aggregation have heightened interest in tau-based therapies for dementia. Success of such treatments depends crucially on translation from non-clinical animal models. Here, we present the age profile of the $PLB2_{Tau}$ knock-in model of fronto-temporal dementia in terms of cognition, and by utilising a directly translatable magnetic resonance imaging approach. Separate cohorts of mice aged 3, 6 and 12 months were tested in an object recognition protocol interrogating visual, spatial, and temporal discrimination in consecutive tests. Upon completion of their behavioural testing, animals were recorded in a 7 T MRI for brain structural integrity and diffusion tensor imaging (DTI) analysis. We report that $PLB2_{Tau}$ mice presented with an age-dependent deficit in novel object discrimination relative to wild-type controls at 6 and 12 months. Spatial and temporal discrimination, though not significantly different from controls, appeared extremely challenging for $PLB2_{Tau}$ subjects, especially at 12 months, since they explored objects less than controls and were devoid of memory. Controls readily recalled all relevant object-related information. At the same time, the T2 weighted voxel-based image analysis revealed a progressive shrinkage of total brain volumes in 6- and 12-month-old $PLB2_{Tau}$ mice as well as relative striatal, but not hippocampal volumes. A regional DTI analysis yielded only reduced mean diffusivity of the fimbria, but not CA1 or dentate gyrus, amygdala, cingulate cortex, or corpus callosum. These data confirm the $PLB2_{Tau}$ mouse as a translationally useful model for dementia research and suggest the importance of the hippocampal input as a determinant for novel object discrimination.

1. Introduction

Despite some progress concerning the basic understanding and mechanistic anomalies underpinning neurodegenerative diseases such as Alzheimer's disease (AD), advancement in terms of disease modifying therapies is lagging behind (Cummings et al., 2022; Passeri et al., 2022; Brandt, 2023). Many targets for pharmacological approaches have been considered for AD and related dementias, but so far, no real effective medications are forthcoming (Cummings et al., 2022; Brandt, 2023). The amyloid hypothesis has been reinvigorated by very recent clinical data that have led the U.S. Food and Drug Administration (FDA) to accelerate approval of aducanumab, lecanemab, donanemab three amyloid monoclonal antibodies, for the treatment of AD (McDade et al., 2022; Couzin-Frankel, 2023; 2024; Mahase, 2023; Dyer, 2024). However, aducanumab withdrawal from the market, and rejection of approval for lecanemab by the European Medicines Agency (EMA) due to limited beneficial effects in slowing clinical decline, together with cost and safety concerns (Espay et al., 2024), leave open alternative targets of disease modifying therapies (Bazzari and Bazzari, 2022; Couzin-Frankel and Piller, 2022; Cummings et al., 2022; Brandt et al., 2023; Moore et al., 2023).

Although far less investigated, Tau aggregation has become a promising target by recent clinical data. The Tau protein aggregation inhibitor, hydromethylthionine (HMTM), a reduced form of methylene

* Correspondence to: University of Aberdeen, Institute of Medical Sciences, Foresterhill, Aberdeen, Scotland AB25 2ZD, UK.
E-mail address: g.riedel@abdn.ac.uk (G. Riedel).

https://doi.org/10.1016/j.brainresbull.2024.111161
Received 18 August 2024; Received in revised form 28 November 2024; Accepted 4 December 2024
Available online 5 December 2024

blue, has been shown to attenuate clinical decline over a one-year period of exposure without safety issues (Wilcock et al., 2018; Wischik et al., 2022). However, other Tau-targeted candidates (antibodies, small molecules, anti-tau antisense, vaccines) enrolled in clinical trials raised safety concerns that need to be considered (Mullard, 2021). These failures in clinical success have been blamed on the lack of suitable animal models, which all only recapitulate some elements of the disease, but do not provide phenotypes matching the human patients. Nowadays, most transgenic rodent models based on the expression of the human mutant tau (hTau) gene bear high hTau expression due to multiple gene copies, highly active and widespread expression of regulatory elements, and display gross behavioural phenotypes (Ramsden et al., 2005; Koss et al., 2016; Ahmed et al., 2017; Gamache et al., 2019; Yokoyama et al., 2022).

Pathological, biochemical, physiological and cognitive endpoints assessed in these models have recently been extended by brain imaging including positron emission tomography (PET, Platt et al., 2011b, Welch et al., 2013) and high-field magnetic resonance imaging (MRI: see Ni, 2021 for review). These non-invasive techniques including volumetric (Holmes et al., 2017; Fung et al., 2020) or functional connectivity analyses (Degiorgis et al., 2020) offer added translational value to these transgenic mouse models with the most valuable observations derived from longitudinal investigations to follow the progression of the disease (Green et al., 2019; Ma et al., 2019). Yet, T2-weighted anatomical MRI or diffusion tensor imaging (DTI) results have not yet led to a homogenous picture about Tau adverse effect on brain integrity (Sahara et al., 2014; Colgan et al., 2016; Massalimova et al., 2020; Ni, 2022).

We have developed a Knock-in (KI) hTau mouse presenting with phenotypes reminiscent of fronto-temporal lobe degeneration (Platt et al., 2011a; Koss et al., 2016). The genetic construct was intended to lead to low expression of human mutated (P301S, R406W) microtubule associated protein Tau based on a single gene knocked into the HPRT locus. Compared to other models with heavy hTau expression (Ramsden et al., 2005; SantaCruz et al., 2005) this would provide a more physiological background for the transgene expression and the progressive development of tau pathology (Koss et al., 2016; Hull et al., 2019; 2020). Phenotypically, $PLB2_{Tau}$ mice present with elevated anxiety and anhedonia already at 6 months of age but show reduced overall activity and cognitive scores in a task taxing semantic properties but not for spatial information (Koss et al., 2016). A further investigation is warranted given that several of these phenotypic features have a likely source in the abnormal processing of prefrontal cortex and/or hippocampus as suggested by *in vivo* electrophysiological recordings (Koss et al., 2016). They include knowledge-based representations and memory formation, and a richer understanding of the brain system contributing to these deficits is therefore one of the aims of this study. In terms of cognitive tasks, we opted for object recognition as it carries both semantic properties (e.g., distinctiveness, familiarity, schema-like knowledge) (Harkotte et al., 2022; Pandya et al., 2024) and episodic-like memory components (Chao et al., 2022; Huston and Chao, 2023). Object recognition was conducted as a spontaneous exploration of various objects displayed in an otherwise familiar environment and memory is inferred by a greater time spent exploring the novel rather than a familiar item. We implemented different versions of object recognition to interrogate separately in the same animal the "what", "where" and "when" components of episodic-like memory (Eacott and Norman, 2004; Kinnavane et al., 2015; Chao et al., 2022; Huston and Chao, 2023) similar to previous studies on 3xTg AD mice (Davis et al., 2013a, b). Here, object recognition was followed by brain scanning using magnetic resonance imaging to explore regional integrity and to reveal potential microstructural alterations that could explain the cognitive deficits. Volumetric MRI and DTI in $PLB2_{Tau}$ mice sought to reveal progressive age-related brain alterations that parallel deficits in properties of episodic-like memory. Indeed, age-dependent behavioural traits in object discrimination were coincident with striatal atrophy and a decrease in mean diffusivity in the fimbria/fornix of 6 and 12 month-old $PLB2_{Tau}$ mice.

2. Materials and methods

2.1. Animals

The creation and breeding regime of $PLB2_{Tau}$ mice have been detailed previously (Koss et al., 2016). In brief, mice originated from a C57BL/6 J background carrying a construct of the full-length human APP and Tau genes under the CAMKII regulatory element in the HPRT locus ($PLB1_{Double}$, Platt et al., 2011a). These mice were crossed with Cre deleter-mice to remove the APP gene on the flanking flox sites leaving a single gene variant containing only hTau with double mutations at P301S and R406W in order to amplify pathology. Founders were crossed to homozygosity and expanded in multiple isolators at positive pressure at a conventional breeder (Harlan, UK – now Inotiv) and aged in this protected housing. All animals derived from homozygous breeding pairs of PLB_{WT} male and $PLB2_{Tau}$ female mice respectively, were homozygous males. Given the tau mutant transgene was knocked into the HPRT locus, which is located on the X chromosome, all male mice positive for human tau are hemizygous/homozygous. By contrast, female PLB2Tau mice are embryonically affected by X chromosome inactivation (lyonization, a key developmental process to compensate for the imbalances in dosage of X chromosomal genes expressed in females relative to males: Patrat et al., 2020) which generates a mosaic expression in cells with different content of the transgenic allele. This also affects the HPRT gene (and the tau transgene) and these inactivation ratios are a strong predictor of population X-chromosome inactivation variability between species and the heterozygosity is amongst the most variable in mice (Werner et al., 2024). Animals were maintained on a free-feeding weight with *ad libitum* access to food and water and a normal day night cycle (lights on from 7am to 7pm, temperature 21 ± 1°C, relative humidity 40–55 %). They were housed in small groups of siblings (<5 subjects) in Macrolon II cages during ageing in a specific pathogen free environment and maintained in these groups during experiments (unless fighting occurred making single housing necessary – 3 wildtype mice). These individuals were consequently removed from the study. Once close to their testing age (3 months, 6 months and 12 months), animals were shipped to the Institute of Cognitive and Integrative Neurosciences of Aquitaine (INCIA) facility (air), University of Bordeaux, Talence. Mice maintained in the same group setting were acclimatised in polycarbonate standard cages Type III; (Tecniplast, Limonest, France), provided with wood shavings (SAFE, Augy, France), cardboard tubes and paper wool as enrichment, and a stainless-steel wire lid. They were housed in climatised rooms with constant airflow, controlled temperature (22°C ± 1°C; humidity 55–60 %), and a 12:12 hour light-dark cycle (lights on at 7 am). Food and water were provided *ad libitum*. Animals were housed in these conditions for 2–4 weeks until behavioural experiments commenced.

At the MRI unit, which was closed to the INCIA, the animals were housed in the same conventional conditions maintained at 21°C ± 1°C, 55 % ± 10 % humidity, in a 12 h light–dark cycle and free access to food and water. Animal pairings were retained during transport and while in this holding facility and a 7-day acclimatisation period was observed.

Experimental outline: Following acclimatization at the INCIA, behavioural experiments were performed during the light phase between 9 am and 3 pm. The running order was counterbalanced with respect to genotype but not blinded due to weight differences between controls and $PLB2_{Tau}$ (see Results). Different cohorts were recorded for 3 weeks (Fig. 1 A). Once behavioural testing was completed, animals were transferred to (truck) and habituated for 7–10 days at the centre of magnetic resonance and biological systems, University of Bordeaux. Magnetic resonance imaging (MRI; for details see below) proceeded for up to 5 days per cohort followed by sacrifice (formalin perfusion under terminal anaesthesia (pentobarbitone)) and tissue harvest for histopathological analysis (not shown).

All experiments were conducted according to the ARRIVE 2.0 guidelines (Percie du Sert et al., 2020) and were ethically approved by a

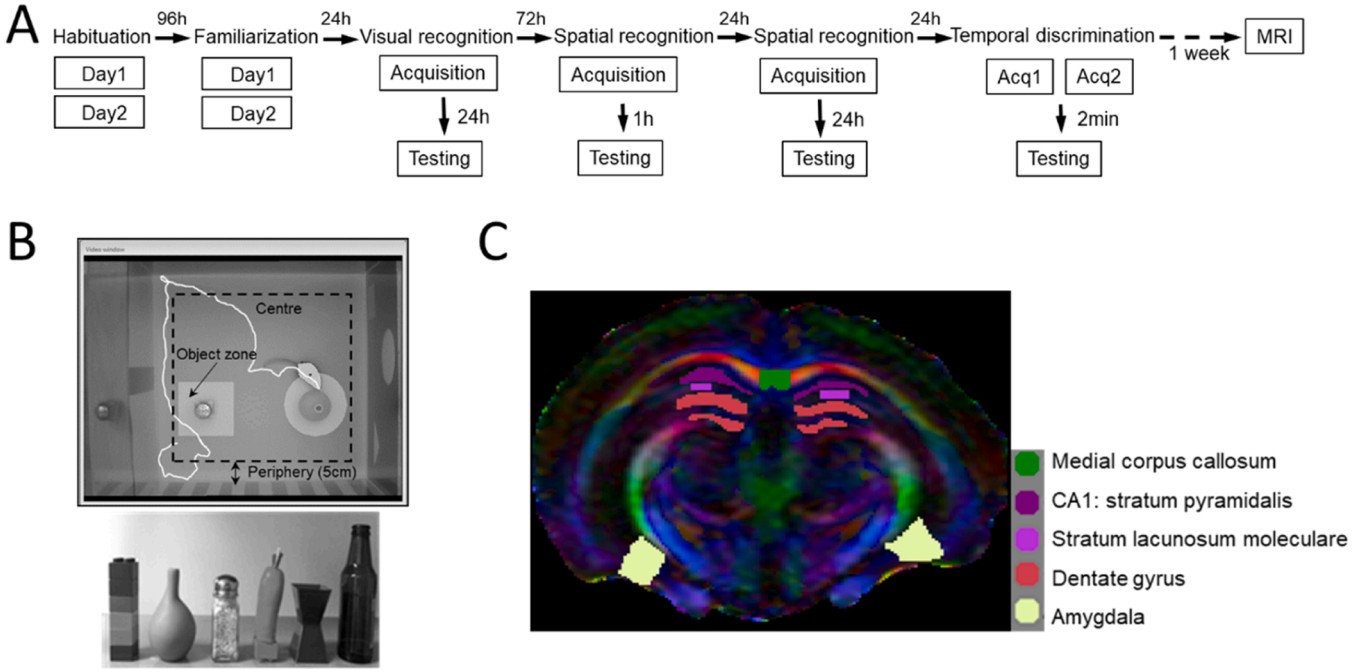

Fig. 1. (A) Diagram outlining the study design for each age cohort. The behavioural testing sequence lasted three weeks followed by MR imaging for 1 week; no testing was performed on weekends. It also indicates the sequence of testing with novel object discrimination first, spatial recognition with two retention intervals (1 h and 24 h) followed by temporal discrimination. (B) Zonal arrangement of the arena with objects. Top: picture of the arena with zone definitions. The arena was empty during habituation, and for object familiarization an object was placed along a midline of the arena at 15 cm from the north wall. The area around the objects symbolises the zone defined for object exploration (nose point within 2 cm around the object). Bottom: samples of objects used in the experiments. (C) Cross section through the mouse brain with anatomical delineations of the different regions of interest (ROIs). Example represents recording of a fractional anisotropy (FA) parametric map at the level of the dorsal hippocampus.

local ethics review board (project licence n° 5012072-A) adhering to the standards outlined in the European Communities Council Directive (63/2010/EU). This is an exploratory study, for which no power calculation was performed a priori.

Age cohorts were run at different time points dependent on availability and randomised for sequence of testing. A total of 65 mice were tested from three different age cohorts: 10 PLB_{WT} and 10 $PLB2_{Tau}$ at 3 months of age; 11 PLB_{WT} and 9 $PLB2_{Tau}$ at 6 months of age; 12 PLB_{WT} and 13 $PLB2_{Tau}$ at 12 months of age. Due to technical issues, these numbers may vary for different experiments. Consequently, group sizes are indicated for each experimental figure.

2.2. Behavioural testing: object recognition

The behavioural test selected was based on object recognition, a spontaneous behaviour based on rodent's natural preference for novelty. Time spent to explore the novel or familiar object was recorded and used to assess memory (Ennaceur and Delacour, 1988; Davis et al., 2013a, b; Kinnavane et al., 2015; Chao et al., 2022). Based on this global behavioural protocol, several variations were designed to interrogate the different components of episodic-like memory (see below). Episodic memory has been shown to be particularly sensitive to neurodegenerative diseases including Alzheimer's disease and frontotemporal dementia (Cummings et al., 1998; Carlesimo and Oscar-Berman, 1992; Hornberger and Piguet, 2012; Poos et al., 2018).

2.2.1. Apparatus and procedures

2.2.1.1. Apparatus and software. All experiments were conducted under dim white light (30 Lux) in an open field (40 x 40 cm) with white Perpex floor, surrounded by grey Perpex walls (25 cm high) decorated with cues (see Fig. 1B). Responses of the animals (locomotor activity, animal location, object exploration) were recorded via an overhead CCTV camera connected to a personal computer running the Any-Maze video-tracking software (Ugo Basile, Varese, Italy). The video tracking system was adjusted to track three points on the mouse (nose, centre of gravity and back of the mouse at its tail) allowing to differentiate the head and its direction from the back of the mouse. Movements were tracked at 10 samples/s in different virtual zones of the arena defined through the software program (Fig. 1, for details see below). Object exploration was recorded when a mouse was directing its nose to an object at a distance of 2 cm or less (object zone). Based on pilot experiments we selected ten duplicate objects that had different shapes (dimensions approximately 15 ×4×4 cm) and varied in colour and material (plastic, glass or metal). Object pairings for testing were selected by similar exploration times scored during pilot experiments and new sets of objects were used for each experiment. Target objects were counterbalanced for genotypes and age cohorts. Arena and objects were wiped with 50 % ethanol solution between each mouse.

2.2.1.2. Procedures. The timeline of behavioural testing is summarized in Fig. 1 A. The three age groups of mice were assessed through independent studies containing the same sequence of behavioural testing sessions. These included habituation, object familiarization, novel object recognition, spatial object recognition and temporal object recognition. One hour prior to each session animals were individually placed in a fresh transfer cage containing only the habitual bedding (wood shavings) and were moved to a waiting room next to the testing room.

2.2.2. Object recognition

2.2.2.1. Habituation. Mice received two daily 10-min habituation sessions to the empty arena. Recordings were used to analyse novelty induced behavioural traits for each genotype. At the start, mice were gently placed at the middle of the front wall with their heads toward the wall. A thigmotaxis zone (outer 5 cm) and an inner central zone were

defined to evaluate aspects of anxiety-like behaviour (see Fig. 1B).

Two measures were extracted from the tracking software program: total distance travelled (cm) in the arena as an index of activity, and time spent in the centre/periphery (s) as proxies for anxiety. For each parameter, the analysis was carried out on data averaged over both sessions.

2.2.2.2. Object familiarization. Two daily sessions were administered to habituate mice to objects in the arena. Mice were allowed to freely explore an object placed in the centre of the chamber for 10 min. The time spent to explore the object was recorded as object exploration. Data were averaged over both sessions.

2.2.2.3. Novel object recognition. Evaluation of episodic-like memory components (what, where, when) began with the object discrimination task to explore the "what" component. During the sample phase, animals were allowed to freely explore two identical copies of an object for 10 min. Novel object recognition was tested 24 h later, wherein each mouse was returned to the same chamber for 5 min exploration (Fig. 2A). During testing we presented one sample object and one novel object placed at the original locations.

Time spent exploring each object (s) and the total distance travelled (cm) in the open field were recorded for subsequent data analysis. A discrimination ratio was defined as time (s) of novel object exploration relative to the total time spent exploring both objects.

2.2.2.4. Spatial object recognition. The spatial component ("where") of episodic-like memory was assessed with two retention delays (1 h and 24 h). Mice were released facing the middle of the west wall at the sample phase and the north wall for the test phase. During the sample phase two sets of identical objects were presented to the animals for 5 min (1 h delay) or 10 min (24 h delay; see Fig. 2B). During the one-hour intersession interval mice remained in the waiting room, a small room contiguous to the experimental room. At the longer delay mice were returned to their home cages and holding rooms. For the test phase one object of each pair was displaced as shown in Fig. 2B and mice were tested for 5 min of free exploration in the arena.

As for novel object discrimination, the time (s) spent exploring each object and the total distance travelled (cm) in the arena were recorded as proxies. A spatial discrimination ratio was computed as time spent with the displaced objects relative to the total exploration time of all objects.

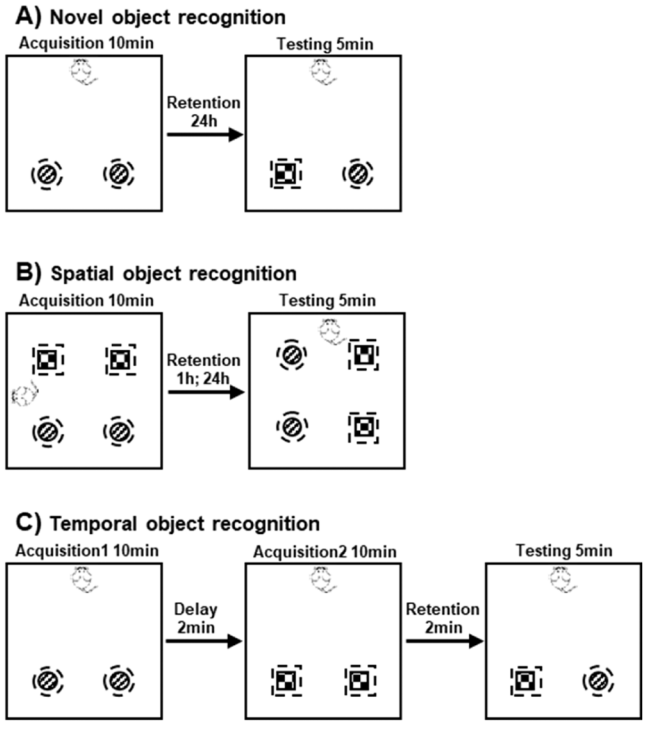

Fig. 2. Schematic diagrams of the novel (A), spatial (B) and temporal (C) object recognition. Starting positions of the mice are indicated at the middle of the north wall with the exception of spatial object recognition where starting positions changed to the west to avoid non spatial biases. Note that for spatial recognition, mice were submitted to a 5 min and a 10 min acquisition session for the 1 h and 24 h retention intervals respectively. The inter-session intervals were selected to explore short- and long-term memory processing. Different objects are indicated by different symbols.

2.2.2.5. Temporal object recognition. Next, we assessed the temporal component ('when') of episodic-like memory. Mice were again released at the middle facing the north wall. The sample phase consisted of two 10 min sessions separated by a 2 min interval. In each session, a different pair of identical objects (objects 1 first, objects 2 second - see Fig. 2C) were presented and after a further interval of 2 min, subjects were placed back into the arena with one object from each pair. The test phase lasted 5 min.

From the video recording, Any-Maze extracted the times spent in the vicinity of each object. A temporal discrimination index was calculated as the ratio of time of exploration of remote object 1 relative to the total exploration time of both objects; ratios $> .5$ were expected to reveal poorer recognition of the remotely presented object 1 relative to the more recent object 2 (interpreted as recency effect).

2.3. Magnetic Resonance Imaging (MRI): acquisition and analysis

In vivo MRI was performed on each age group: 3, 6 and 12 months. A 7 T Bruker BioSpin scanner (for 30dpi) was used. Mice were kept under gaseous anaesthesia (isoflurane, 3 % for induction and 2 % for maintenance in 1.5 L/min of synthetic air) and placed over a heating pad to maintain body temperature. A T2-weighted (TR/TE = 5000/10 ms, NEX = 2, FOV=20 x 16 mm, matrix = 102 x 80, slices = 25, slice thickness = 0.3 mm, no interval, resolution = 102 x 82 x 300 μm) was acquired first; and a high resolution/sensitivity diffusion MRI pulse sequence (TR/TE = 1300/46 ms, 30 directions, bmax = 1000 s/mm^2, FOV = 16 x 12 mm, matrix = 196 x 148, slices = 25, slice thickness = 0.469 mm, no interval, resolution = 82 x 81 x 469 μm) with a 3D sampling of Fourier-space (Tounekti et al., 2018; Crombé et al., 2022) was used in this study to compute Diffusion Tensor Imaging (DTI).

Parametric maps for T2-weighted recordings were processed using MIPAV Software (https://mipav.cit.nih.gov/). Regions of interest (ROIs) were outlined on the T2 images using anatomist of the suite BrainVisa (http://brainvisa.info/web/index.html) to calculate volumes for (i) total brain; (ii) hippocampus; (iii) striatum.

Visual quality control of the DTI images was performed; direction of diffusion by direction to evaluate movement and ghosting artefacts using MIPAV software. Diffusion images with poor quality were removed from the data, four maximum diffusion directions were discarded. FSL 5.0 (https://fsl.fmrib.ox.ac.uk/fsldownloads_registration, Analysis Group, FMRIB, Oxford, UK) was used to process DTI images and to create a mask for the entire brain. Eddy current correction was applied, and the DTI parametric maps were created (Mean Diffusivity (MD), Fractional Anisotropy (FA), first to third eigenvalue (λ1 - λ3)). Six different ROIs were manually delineated on the coronal color-coded FA maps for each mouse. Three sections were selected for outlining ROIs when both the Corpus Callosum and the dorsal hippocampus were clearly distinguished and anatomical delineations included: CA1, dentate gyrus, amygdala, anterior cingulate cortex (at the edge of the olfactive bulb), medial Corpus Callosum and medial fimbria. Each DTI parameter was extracted from these 6 ROIs.

On a subset of data, two experimenters blind to phenotypes delineated ROIs on T2 and on FA maps to check for consistencies of the

boundaries used (see example of FA map in Fig. 1 C). On this subset (n = 26), coefficient correlation between the two experimenters reached at least 0.85.

2.4. Statistical analyses

Data are expressed as mean + SD. Statistical analyses were conducted using Statview 5.01 (SAS Institute Inc.). Normality was confirmed according to Kolmogorov-Smirnov so that genotype and age effects on behaviour were analysed using one- or two-way Analysis of Variance (ANOVA), followed when appropriate, by *post hoc* comparisons (Fisher's PLSD). Between-genotype comparisons by age range applied Student's *t*-test. In addition, with quantitative variables, the effect size measures were interpreted using Cohen's rules of thumb, where "d" value of 0.20 represents a small effect, around 0.50 a medium size effect, and 0.80 or higher a large effect size (Cohen, 1988). To gain insight into individual group performances, we compared the discrimination index to the theoretical mean of 50 % (corresponding to equal exploration of both altered and stable object) using a one-sample *t*-test. MRI data were analysed using one- or two-way ANOVA (genotype by age), followed by *post hoc* comparisons when appropriate. In all instances, values of $p < 0.05$ were considered as statistically significant. Only significant differences are reported for clarity.

3. Results

3.1. $PLB2_{Tau}$ mice are smaller than controls

Mice have been weighed regularly during handling and testing sessions. As shown in Fig. 3A, the mean body weight was significantly lower in the 3 cohorts of $PLB2_{Tau}$ mice relative to their age-matched PLB_{WT} (2-way ANOVA: main effect of genotype: $F(1,59) = 72,5$; $p < 0.0001$; main effect of age: $F(2,59) = 21.3$; $p < 0.0001$; for age-wise comparison, see asterisks in Fig. 3A). Intriguingly, there was no weight gain during ageing in $PLB2_{Tau}$ mice ($F(2,29 = 2.9$; $p = 0.07$). Yet, wild-type control mice gained significant weight with age ($F(2,30 = 22.45$; $p < 0.0001$) and this difference was also returned in the two-way ANOVA in the interaction between age and genotype ($F(2,59) = 7.16$; $p = 0.0016$).

As a corollary, structural MRI showed smaller brain volumes in $PLB2_{Tau}$ mice relative to PLB_{WT} at all ages ($F(1,47) = 49.6$; $p < 0.0001$; Fig. 3B, for age-wise comparison, see asterisks) and only PLB_{WT} mice increased brain volumes with age ($F(2,23) = 6.4$; $p = 0.006$), but not $PLB2_{Tau}$ ($F<1$).

3.2. Genotype comparisons during open field and object habituation

As illustrated in Fig. 4A, genotypic differences were observed in locomotor activity during the two habituation sessions. This was confirmed by a two-way ANOVA yielding a significant age x genotype interaction ($F(2,59) = 6.06$; $p = 0.004$). The 3-month old $PLB2_{Tau}$ mice exhibited a much higher locomotor activity compared to PLB_{WT} ($t(18) = 2.67$; $p = 0.016$, Cohen's $d = 1.2$) whereas the opposite was observed for the 12-month old mice ($t(23) = 2.24$; $p = 0.035$, Cohen's $d = 0.9$). As an index of anxiety, time in centre yielded significant effects of age ($F2,59) = 15.94$; $p < 0.0001$), genotype ($F(1,59) = 5$; $p = 0.03$) and an interaction between these terms ($F(2,59) = 9.68$; $p = 0.0002$). This effect was mainly due to a lower time spent in the centre in the 3-month old $PLB2_{Tau}$ mice compared to controls ($t(18) = 4.66$; $p = 0.0002$, Cohen's $d = 2.1$) (see Fig. 4A). No further differences were observed for the two older age cohorts. As a result, the anxiety trait of the $PLB2_{Tau}$ mice shown in a previous report (Koss et al., 2016) was not replicated in these experimental conditions.

Familiarisation recorded as time with head directed towards the object in its immediate vicinity also returned a reliable effect of age ($F(2,58) = 11.55$; $p < 0.0001$), of genotype ($F(1,58) = 6.28$; $p = 0.02$) and an interaction ($F(2,58) = 11.15$; $p < 0.0001$). Detailed genotype comparison for the different age ranges confirmed a dramatic reduction of object exploration in 12-month old $PLB2_{Tau}$ mice compared to PLB_{WT} ($t(23) = 5$; $p < 0.0001$, Cohen's $d = 2$) and no noticeable differences when younger cohorts were examined (Fig. 4B). In contrast to the findings during habituation to the open field, the discrete anxiety phenotype in the $PLB2_{Tau}$ mice did not transfer to the object exploration phase, particularly in the older animals. Although the two-way ANOVA confirmed significant effects of age ($F(2,59) = 26.36$; $p < 0.0001$) and genotype ($F(1,59) = 11.16$; $p = 0.002$) but no interaction ($F(2,59) = 1.1$; ns), on time in centre as anxiety criterion, post-hoc comparisons showed significantly reduced time spent in centre only in 3 m old $PLB2_{Tau}$ mice ($t(18) = 3.17$; $p = 0.005$, Cohen's $d = 1.42$), but not older cohorts Clearly, there was no consistent phenotype for object exploration in $PLB2_{Tau}$ mice. This is an important prerequisite for object recognition testing.

3.3. Object recognition

In the following, mice of all age cohorts underwent a series of object recognition tests tailored to interrogate for the 'what', 'where' and 'when' of episodic-like memory.

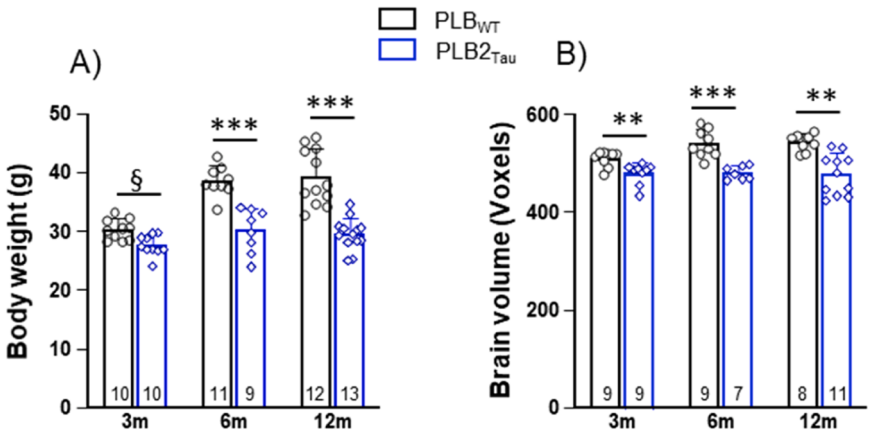

Fig. 3. A) Body weight and B) Brain volume of $PLB2_{Tau}$ and PLB_{WT} mice at the three age groups tested. While there was considerable weight and brain volume gain in PLB_{WT} mice as they aged, this was not seen on $PLB2_{Tau}$ animals. N for each group is indicated in each bar. Data represent Mean + SD and individual data scatter; for details on statistics, see text. § = p = 0.06; * * = $p < 0.01$; * ** = $p < 0.001$ (*t*-test).

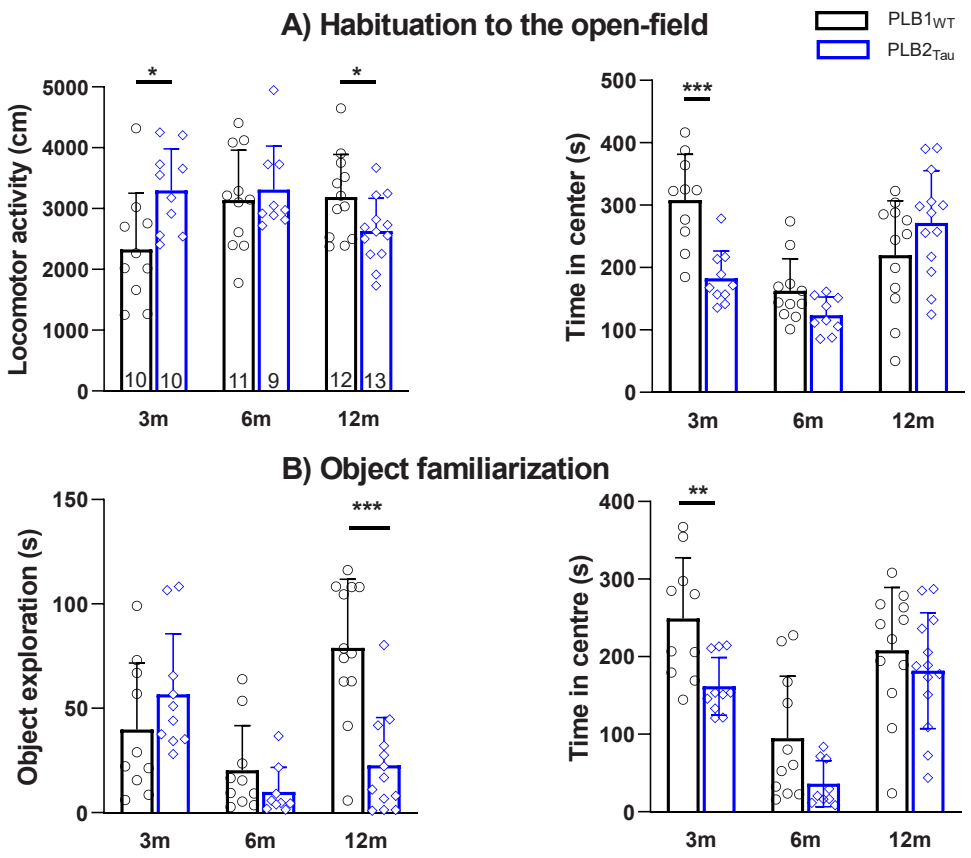

Fig. 4. Ambulation and zonal exploration during habituation. A) Locomotor activity (left) and time spent in the centre (right) of the open field during the two sessions of habituation were measured in the $PLB2_{Tau}$ and PLB_{WT} mice at the three age groups. B) Object exploration and time spent in the centre (right) were recorded during the two object familiarization sessions in both genotypes of the three ages. Symbols represent individual data scatter averaged over two habituation (A) and object familiarization (B) sessions and bars indicate group means +SD. N's are illustrated in bars of A left. For details on statistics, see text. * $p < 0.05$; * * $p < 0.01$; * ** $p < 0.001$ (*t*-test).

3.3.1. $PLB2_{Tau}$ mice are impaired in novel object recognition

Animals were first tested in novel object recognition to assess the "what" component of episodic-like memory at a retention interval of 24 hours. As shown in Fig. 5 and Table 1, $PLB2_{Tau}$ mice at all ages displayed a lower discrimination score between familiar and novel object than their age-matched controls. The ANOVA confirmed a main effect of age ($F(2,49) = 8.02$; $p = 0.001$) and genotype ($F(1,49) = 11.52$; $p = 0.001$) with no interaction. Since age cohorts were tested individually at different time points, post-hoc *t*-test for the different age groups confirmed a significant difference between genotypes at 6 ($t(18) = 5.7$; $p = 0.03$, Cohen's d= 1) and 12 ($t(14) = 7.3$; $p = 0.02$, Cohen's d= 1.4), but not 3 months (see asterisks in Fig. 5A). As for the time spent in object exploration during the acquisition session (Fig. 5B) no overall differences in genotype or age were observed (F's ≤ 2; p ≥ .16), but a significant genotype by age interaction ($F(2,49) = 4.16$; $p = 0.02$) due to the 6 month cohort was noted. Therefore, the impairment of the 6 month old $PLB2_{Tau}$ mice might be explained by a somewhat reduced object exploration during acquisition ($t(18) = 2.46$; $p = 0.025$, Cohen's

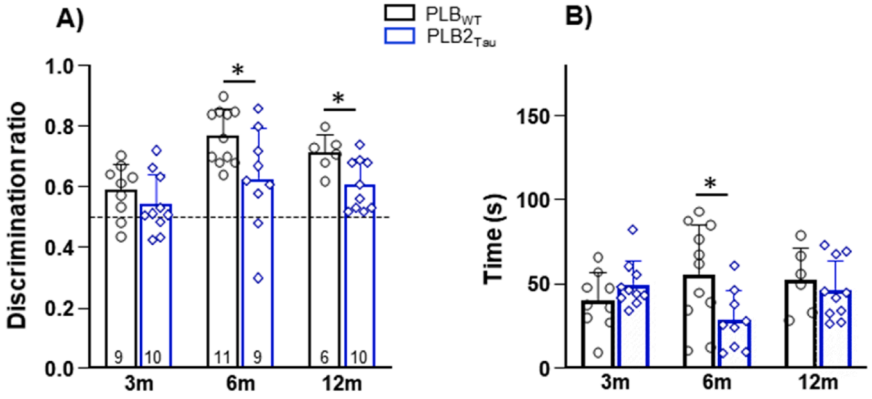

Fig. 5. $PLB2_{Tau}$ mice are impaired in novel object discrimination at 6 and 12 months of age as assessed by the discrimination ratio (A). N's are indicated in bars. Mice were excluded when climbing on the objects. A diminution of time spent to object exploration (B) during the acquisition session was only observed in the 6 month-old $PLB2_{Tau}$ mice compared to PLB_{WT}. Data represent individual animals as scatter and group mean + SD. N's are inserted in bars in A. For details on statistics, see text. * $p < 0.05$ (*t*-test). Dashed horizontal line indicates the level of chance.

Table 1
Statistical analysis (t-tests) of discrimination ratios in the different object recognition phases compared to the theoretical chance level (0.50) in all groups. Impairments in performance of $PLB2_{Tau}$ mice appeared to be strongest in novel object ('what') and temporal ('when') discrimination (see highlights).

Discrimination ratio / chance (p)	Age (months)	Novel Object (ITI: 24 h)	Spatial (ITI: 1 h)	Spatial (ITI: 24 h)	Temporal (ITI: 2 min)
PLB_{WT}	3	*0.02*	*0.045*	0.44; ns	*0.009*
	6	*< 0.0001*	*0.0008*	*< 0.0001*	*0.002*
	12	*0.0003*	*0.007*	*0.024*	*0.002*
$PLB2_{Tau}$	3	0.21; ns	0.10; ns	*0.002*	*0.002*
	6	0.054; ns	*< 0.0001*	*< 0.0001*	0.07; ns
	12	*0.003*	*0.02*	0.64; ns	0.23; ns

d= 1.1). No such differences were observed in the 12-month old cohorts during acquisition ($t(14) = 0.61$; $p = 0.55$). We further sought to confirm object discrimination by comparing the discrimination ratio of each group to the theoretical level of chance (see Table 1, if below 0.5, there is preference for the familiar object, if above, preference for the novel object is established). The predicted outcome of all PLB_{WT} cohorts performing above chance and preferring the exploration of the novel object was verified (p's ≤ 0.018). Although $PLB2_{Tau}$ mice were impaired in the amount of discrimination at 6 and 12 months relative to PLB_{WT}, they nevertheless exhibited some preference for the novel object (p's ≤ 0.054).

Collectively, we take this as evidence for an age-dependent deficit in long-term object recognition memory in $PLB2_{Tau}$ mice.

3.3.2. *$PLB2_{Tau}$ mice present no deficit in spatial object recognition*

Spatial object recognition was conducted next with the intention to probe for the "where" component of episodic-like memory. We discriminated between short-term (1 h) and long-term (24 h) memory intervals between sampling and testing.

3.3.2.1. Short-term memory test at 1 h post-acquisition. As depicted in Fig. 6 no genotype effects were observed for the discrimination ratios. This was substantiated by an overall two-way ANOVA with age and genotype as between subject factors (genotype: $F<1.4$; Fig. 6A) and coincided with similar levels of object exploration between both mouse lines ($F<1$; Fig. 6B). However, there was a significant effect of age in the discrimination ratio ($F(2,59)= 10.05$; $p = 0.0002$) mainly due to better performance in both genotypes at 6 month of age. All groups presented with a discrimination ratio significantly above chance level except for the 3 month-old $PLB2_{Tau}$ mice which nevertheless also showed some trend (Table 1).

3.3.2.2. Long-term memory test at 24 h post-acquisition. We next implemented a longer memory interval of 24 h to tackle long-term memory processes. Data are summarised in Fig. 7. Similar to the data for short-term memory, the discrimination ratios did not differ between $PLB2_{Tau}$ and PLB_{WT} mice ($F<1$), yet a main effect of age underlined the impression of different age-related retention levels ($F(2,59)= 31.7$; $p < 0.0001$; Fig. 7A). This again appeared to be due mainly to the high performance of the 6-month-old cohorts.

In contrast to the discrimination ratios, time exploring the objects during acquisition returned a genotype x age interaction ($F(2,59)= 5.676$; $p = 0.006$; Fig. 7B) and a main effect of age (($F(2,59)= 16.5$; $p < 0.0001$), but no genotype effect (F's < 1). Multiple comparison between the individual age cohorts then confirmed this interaction with a significantly higher exploration time at 3 months ($t(18) = 3.69$; $p = 0.002$, Cohen's d= 1.6) and a lower one at 12 month ($t(23) = 2.34$; $p = 0.03$, Cohen's d= 0.9) in $PLB2_{Tau}$ subjects. Finally, as suggested by Table 1 for performance levels relative to chance, most age cohorts found the long-term 24 h memory test more challenging (less significance) than the shorter 1 h retention interval, except animals aged 6 months.

3.3.3. *$PLB2_{Tau}$ mice older than 6 months find temporal discrimination most challenging*

We next established a temporal discrimination in an attempt to probe whether animals prefer exploring recently or remotely presented objects. This required two 10 min acquisition sessions followed, after a 2 min interval, by a short 5 min retention test. As summarised in Fig. 8A, all age cohorts presented with a bias for the remotely presented object (discrimination index > 0.5). This recency effect (memory for recently presently object intact) seemed to be similar for both PLB_{WT} and $PLB2_{Tau}$ mice since the factorial comparison did not yield any reliable differences (F's < 1,8). Nevertheless, it appears that $PLB2_{Tau}$ subjects aged 6 month or older struggled to retain task-specific information as they were not different in performance from chance (Table 1), whereas $PLB1_{WT}$ mice were still highly biased towards the remote object.

For the two 10 min acquisition sessions, a two-factor ANOVA on object exploration showed a main age effect for acquisition 1 ($F(2,54)= 4.51$; $p < 0.02$; Fig. 8B) and an age x genotype interaction for acquisition 2 ($F(2,54)= 3.53$; $p = 0.04$; Fig. 8C) that was mainly due to a

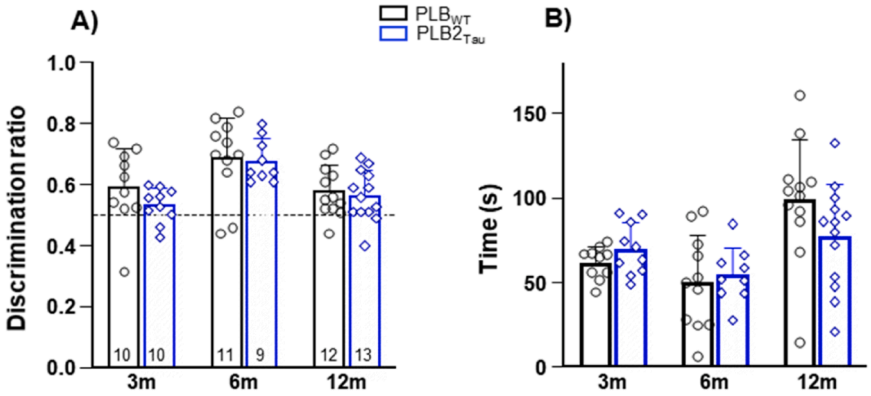

Fig. 6. Short term memory test for spatial object recognition conducted 1 h after sample training. (A) Discrimination ratios were not different between genotypes. Similarly, no differences between genotypes were observed for object exploration (B) during the acquisition session. Data represent individual animals as scatter and group mean + SD. N's are inserted in bars in A. For details on statistics, see text. Dashed horizontal line indicates the level of chance.

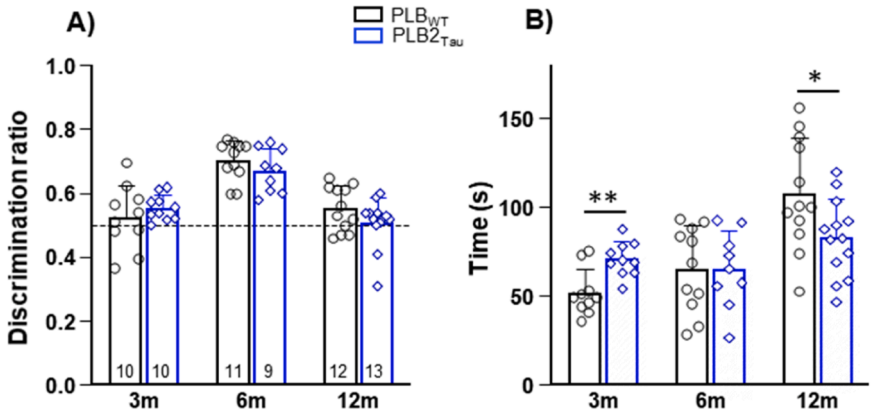

Fig. 7. Long-term spatial object recognition recorded 24 h after acquisition. No genotype effect was found for discrimination ratios (A) at any age. (B) Object exploration during acquisition differed between genotypes at 3 and 12 months. Data represent individual animals as scatter and group mean + SD. N's are displayed in bars of A. For details on statistics, see text. * = $p < 0.05$; * * = $p < 0.01$ (*t*-test). Dashed horizontal line indicates the level of chance.

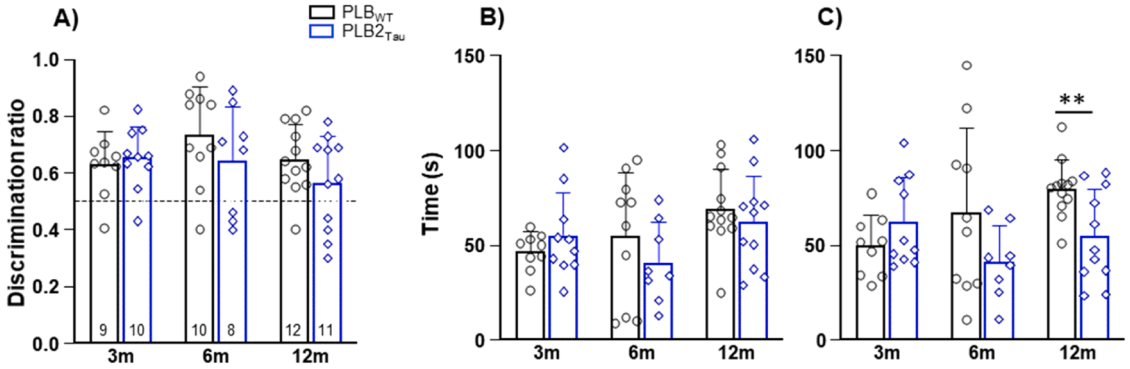

Fig. 8. Temporal discrimination. (A) Discrimination ratios above 0.5 confirmed a recency effect since subjects spent more time in the vicinity of the remotely presented objects. No age and genotype effects were statistically substantiated. (B) Object exploration during acquisition 1 and (C) during acquisition 2. A significantly lower exploration time for acquisition 2 at 12 months was confirmed in PLB2$_{Tau}$ mice. Data represent individual animals as scatter and group mean + SD. N's are indicated in A. For details on statistics, see text. * * $p < 0.01$ (*t*-test). Dashed horizontal line indicates the level of chance.

significantly heightened object exploration level in 12-month old PLB$_{WT}$ mice ($t(21) = 2.98$; $p = 0.007$, Cohen's d= 1.2). Again, the amount of object exploration did not seem to predict the level of performance in temporal discrimination as confirmed by an overall regression analysis (R=0.204; $p = 0.12$; not shown).

3.3.4. *Object exploration deficits in PLB2$_{Tau}$ mice is age-related*

For multiple phases of object exploration, we noticed small differences between PLB$_{WT}$ and PLB2$_{Tau}$ mice (see Figs. 5–8). These conveyed the impression that older PLB2$_{Tau}$ animals aged 6 and more so at 12 months explored objects less than their wildtype counterparts. An average for each animal across all sample trials was calculated (Fig. 9). The two-factor ANOVA confirmed a significant main effect of age ($F(2,59) = 8.66$; $p = 0.0005$) with an age x genotype interaction ($F(2,59) = 5.05$; $p = 0.001$) but not for genotype ($F(1,59) = 2.51$, $p = 0.12$). Main effects were due to a higher level of object exploration at 3 ($p = 0.02$, Cohen's d=1.17) and a lower level at 12 months in PLB2$_{Tau}$ mice ($p < 0.01$, Cohen's d=0.74) relative to PLB$_{WT}$. No phenotype occurred at 6 months. Altogether, these data confirm the overall activity during the habituation stage and underline an inversion of heightened activity at young and reduced activity at old age in PLB2$_{Tau}$ subjects.

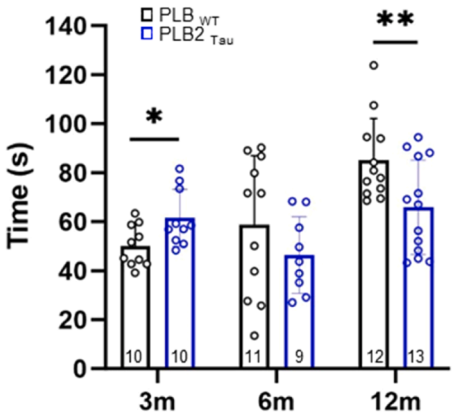

Fig. 9. Average of exploration times from all sample trials for each animal (scatter and Mean + SD) across 3 age groups. In PLB2$_{Tau}$ animals, times for exploring the objects was higher in young (3 m), not different in middle aged (6 m) and reduced in old (12 m) subjects. N's are indicated in bars. For details on statistics, see text. * $p \leq 0.05$, * * $p \leq 0.01$ (*t*-test).

3.4. *Brain imaging*

3.4.1. *Progressive age-related atrophy of the striatum in PLB2$_{Tau}$ mice*

High resolution T2-weighted structural imaging was applied to investigate the morphometric phenotype of the PLB2$_{Tau}$ model in comparison to their respective PLB$_{WT}$. The smaller brain of PLB2$_{Tau}$ mice (see Fig. 3B) required normalization of the data to detect potential alterations in selected ROIs that were not merely due to a general reduction of brain size. Areas critically engaged in recognition memory in

rodents are both hippocampus and striatum (Chao et al., 2022) which guided our selection of ROIs. Fig. 10 represents the outcome of this analysis. As expected for lateral ventricles (Fig. 10A), their volume increased with age ($F(2,47)= 6.04$; $p = 0.005$) due to general brain atrophy in a genotype independent manner. A progressive age-related reduction of striatal volume was observed in $PLB2_{Tau}$ mice while the volume of striatum remained stable in PLB_{WT} (Fig. 10B). The two-way ANOVA confirmed this observation by returning a significant main effect of genotype ($F(1,47)= 9.32$; $p = 0.004$), of age ($F(2,47)= 8.17$; $p = 0.001$) but no interaction ($F<1$). The genotype effect was mainly due to a significantly reduced striatal volume in 12-month-old $PLB2_{Tau}$ mice relative to age-matched PLB_{WT} ($t(17) = 3.43$; $p = 0.003$, Cohen's $d= 1.6$). We did not observe any genotype or age-related differences in volume of the dorsal hippocampus (Fig. 10C). These data provide compelling evidence for some dementia relevant structural brain changes in $PLB2_{Tau}$ mice that occur in an age-dependent and progressive manner and are most obvious in 12 month old subjects.

3.4.2. Diffusion tensor imaging reported deficits in diffusion of fimbria inputs to hippocampus

DTI was used to detect changes in white and grey matter microstructures. Based on our previous behavioural and electrophysiological data (Koss et al., 2016) we selected a series of brain regions that were related to mnemonic and anxiety-related processes, mostly hippocampal and amygdala structures. (Table 2). Reduced Mean Diffusivity (MD) was suggested and confirmed statistically (effect of genotype: $F(1,54)= 12.75$; $p = 0.001$) only for the fimbria, but no other ROIs. Post-hoc comparisons yielded a significant reduction of MD in the fimbria in 6- and 12-month-old $PLB2_{Tau}$ mice compared with PLB_{WT} (Fisher's PLSD: $p \leq 0.013$) suggesting a microstructural modification of hippocampal input from the cholinergic basal forebrain (Drever et al., 2011; Deiana et al., 2011; Marighetto et al., 1994a,b; Scullion et al., 2019). In addition to these genotype differences, however, a consistent age-related reduction in MD was observed for all ROIs (p's ≤ 0.01).

4. Discussion

4.1. Subtle deficits in recognition memory in $PLB2_{Tau}$ mice

The central tenet of this paper was to further characterise $PLB2_{Tau}$ mice as a putative and physiologically relevant experimental rodent model mimicking core symptoms of behavioural variant frontotemporal dementia (bvFTD) (Koss et al., 2016). Since previously reported and characterised tau mice (see https://www.alzforum.org/research-models/) containing mutations at position 301 in exon 10 were based on high expression levels of tau coincident with sensory-motor impairments (Ramsden et al., 2005; SantaCruz et al., 2005; Takeuchi et al., 2011; Mellone et al., 2013; Kubota and Kirino, 2021), a more physiological model is required with a disease relevant age-related progression of tau pathology. Therefore, $PLB2_{Tau}$ was developed (Platt et al., 2011a; Koss et al., 2016; Hull et al., 2019; 2020) by selective knock-in of the human tau gene into the *HPRT* locus with neuronal expression under the Thy1 regulatory element, and age-dependent profiling was attempted here. In line with deficits in bvFTD patients (Ahmed et al., 2017; Poos et al., 2018; Wong et al., 2018), episodic-like memory in rodents was scrutinised, and both anatomical and physiological underpinnings were determined in mice (Chao et al., 2022). In our sequential analysis of object recognition tests probing the different (what, where, when) components of episodic-like memory $PLB2_{Tau}$ mice presented with a clear age-dependent impairment in the novel object discrimination (what), and more subtle deficits in spatial (where) and temporal (when) discrimination protocols. All effects returned a sizable Cohen's d and thus were robust. They were most obvious at 12 months of age. Yet, an unexpected anomaly was observed in that middle aged 6-month-old cohorts performed better throughout all discrimination protocols than younger and older subjects. While mechanistic underpinnings remain elusive, we note that age cohorts were tested at different time points during the year, and that 3 months old mice are still undergoing prefrontal synapse pruning with not fully developed neural mechanisms for learning (Kolb et al., 2012). The lower performance of older animals may be readily ascribed to their ageing process. Of note here is that a similar but not as dramatic age-dependent performance was reported earlier by Ryan et al. (2013) for $PLB1_{Triple}$ and PS1APP (cross between Tg2576 and $PS1_{M146L}$) for spatial learning in the radial arm maze.

It appears from the literature that transgenic rodents (mice and rats) expressing a human tau gene containing the P301S mutation consistently present with deficits in novel object discrimination (Yang et al., 2015, 2017; Ji et al., 2018; Malcolm et al., 2019; Rollins et al., 2019; Camargo et al., 2021; Onishi et al., 2021; Sun et al., 2021; Tong et al., 2022; Perez-Garcia et al., 2023; Wang et al., 2023). Most of these were generated with high-expression regulatory elements such as the Thy1 or prion protein promotor leading to massive, often unphysiologically high tau overexpression already at ages as young as 3–4 months. Other components such as spatial and temporal recognition elements of episodic-like memory, however, remain widely elusive in these tau models and are often compromised due to motor deficits which make the dissociation between exploration and memory performance difficult. In $PLB2_{Tau}$ mice, we here report a genuine age-related gradient of recognition memory failures in both novel object discrimination and temporal

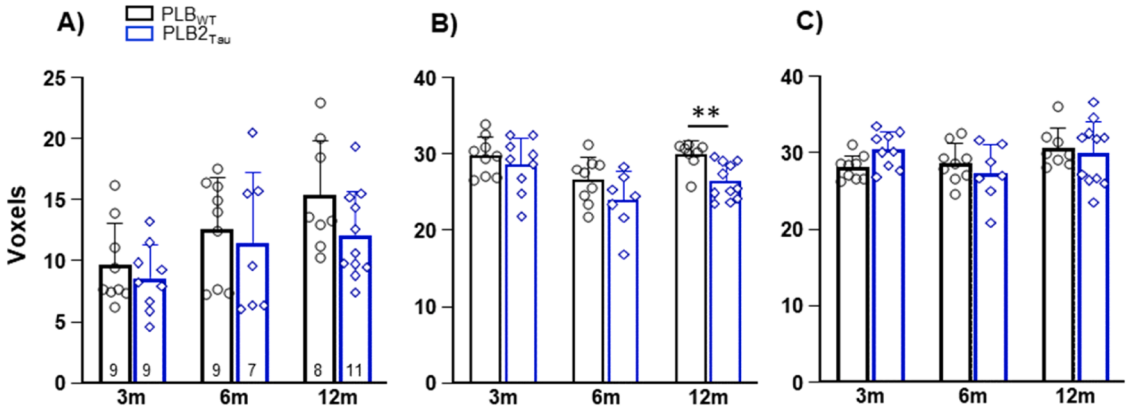

Fig. 10. High resolution T2 weighted structural imaging in $PLB2_{Tau}$ and PLB_{WT} mice. Volumes of brain structures have been normalized to brain volume. (A) Age-dependent increase of ventricle volume appeared in both genotypes. (B) A significant reduction in striatal volume was found in 12 month-old $PLB2_{Tau}$ mice. (C) No volumetric differences appeared for the dorsal hippocampus. Data represent individual animals as scatter and group mean + SD. N's are shown in bars of A. For details on statistics, see text. * * $p < 0.01$(*t*-test).

Table 2
DTI metrics in the selected ROIs. MD (μm^2/ms) is expressed as Mean ± SD. Compared to PLB_{WT} a significant reduction of MD was observed only in the fimbria of 6- and 12-months old $PLB2_{Tau}$ mice (grey highlights with asterisks). For details on statistics, see text. * $p < 0.05$.

DTI MD μm^2/ms	Age (months)	Cingulate cortex	Corpus callosum	Amygdala	CA1	Fimbria	Dentate gyrus
PLB_{WT}	**3**	0.696 ± 0.094	0.705 ± 0.05	0.875 ± 0.151	0.730 ± 0.083	1.168 ± 0.143	0.685 ± 0.078
	6	0.633 ± 0.054	0.637 ± 0.048	0.859 ± 0.176	0.648 ± 0.061	**1.06*±** **0.138**	0.605 ± 0.057
	12	0.559 ± 0.067	0.559 ± 0.059	0.713 ± 0.139	0.544 ± 0.068	**1.04*±** **0.114**	0.509 ± 0.074
$PLB2_{Tau}$	**3**	0.705 ± 0.104	0.705 ± 0.128	0.832 ± 0.216	0.699 ± 0.128	1.121 ± 0.172	0.670 ± 0.118
	6	0.654 ± 0.084	0.645 ± 0.077	0.935 ± 0.26	0.689 ± 0.094	0.901 ± 0.095	0.645 ± 0.095
	12	0.555 ± 0.083	0.541 ± 0.09	0.729 ± 0.184	0.539 ± 0.075	0.888 ± 0.101	0.513 ± 0.08

recognition, especially when discrimination ratios are compared with chance levels; these are akin to the human deficits and present with a clear and progressive ageing process (Hornberger and Piguet, 2012; Poos et al., 2018; Macchitella et al., 2023). Moreover, discrimination between novel and familiar objects constitutes a semantic component of recognition, and the deficits are in line with our previously reported ~~semantic~~ deficit in social transmission of food preference which specifically explores semantic aspects of this associative memory task (Koss et al., 2016) in this $PLB2_{Tau}$ line. We have not observed locomotor impairments or anxiety-related phenotypes in any of our age cohorts. While this appears to contradict our previous report (Koss et al., 2016), recordings were not equivalent, and we here only explored very short test periods (up to 10 minutes) while Koss and colleagues reported much longer timelines (PhenoTyper: days) and very different contexts (elevated plus maze). Therefore, we cannot exclude that locomotor phenotypes would occur in our paradigm in older $PLB2_{Tau}$ subjects subjected to longer test periods. However, the overall lower object exploration in 12-months old $PLB2_{Tau}$ mice cannot account for the memory deficit given the lack of correlation between time spent in object exploration during acquisition and discrimination ratios.

Contrary to novel object recognition, it appears that spatial object recognition has not been investigated in tauopathy mouse models. We used this test, also called object-in-place task, to promote an object-place association that would be more sensitive to hippocampal dysfunction than a simple object displacement in a novel location (Chao et al., 2022). Doing this, the failure to reveal a clear deficit for spatial object recognition corroborates our reported lack of deficit in water maze task (Koss et al., 2016) and suggests that hippocampal function is grossly intact and only a long-term retention interval led to some subtle spatial deficits. The behavioural observation is in line with a recent report showing in the transgenic Tau-P301L mouse model a deficit in novel object recognition without any alteration of spatial memory evaluated in a T-maze spontaneous alternation task and in a water maze task (Camargo et al., 2021). This trait contrasts with other P301S models for which spatial learning deficits in the water maze have been confirmed (Sun et al., 2021; Ji et al., 2018; Wang et al., 2023; see Table 1 in Koss et al., 2016 for review). Many of these P301L/S models presented with normal acquisition learning over multiple training sessions but showed deficits in memory trials. In contrast to the water maze, in which repeated trials over long periods are given, the object-in-place task presents the animal with a trial unique challenge during recall and requires a discrimination between stationary and shifted object. Despite these differences in training protocols, it appears that the $PLB2_{Tau}$ phenotype is thus more akin to other models of non-mutated tau expression (Geiszler et al., 2016; Tulloch et al., 2021; Barendrecht et al., 2023) and intriguingly replicated the findings from 3xTg-AD mice carrying a P301L mutation in their human transgenes (Davis et al., 2013a, b). While we cannot comment on the genetic interactions of the multi-transgenic 3xTg-AD mice, for single transgene expressors, however, we suggest that the discrepancies are due to model generation, insertion sites, regulatory elements and background strains. Unexplored to date in single transgene tau models is the temporal aspect of episodic-like memory (recency task). Here we provide evidence for an age dependent impairment (measured against chance level performance). While control animals show a strong recency effect, $PLB2_{Tau}$ mice aged 12 months present with little bias for either remotely or recently presented objects. Intriguingly, this cohort also had much reduced exploration for the recent objects, a trait that we previously termed motivational deficits or apathy (Koss et al., 2016).

Collectively, these data provide support for the notion that ageing is a major factor for the emergence of behavioural traits in $PLB2_{Tau}$ mice. The subtlety of the spatial deficits seems to predict intact hippocampal function in these animals, and this was confirmed by volumetric and diffusion tensor MRI protocols. Clearly, these behavioural observations corroborate clinical data pointing to a moderate role of the hippocampal formation in the symptomatology in Tau-related bvFTD (Jakabek et al., 2018; Miller and Llibre-Guerra, 2019).

While it appears intuitively reasonable to argue that the gross ambulatory phenotype could be related with an expression of these cognitive deficits in $PLB2_{Tau}$ mice, caution is required as differences in object exploration were not always co-incident with spatial and temporal deficits and a correlation between object exploration duration and cognitive performance was not established here and shown by others (Ameen-Ali et al., 2021; Davis et al., 2013a,b; Dere et al., 2008). We therefore suggest that both activity related and cognitive phenotypes in our $PLB2_{Tau}$ model arise through different mechanisms (for example different brain regions being affected by tau pathology) and some MRI registered anomalies may explain this dissociation.

4.2. A strong striatal MRI phenotype as a biomarker for bvFTD

As the final translational endpoint of this study, structural and diffusion tensor imaging protocols run to explore whether behavioural effects in $PLB2_{Tau}$ mice can be explained by anatomical anomalies. From the core regions selected for analysis, structural MRI reported an age-dependent reduction of striatum volume in $PLB2_{Tau}$ mice, concomitant with increased volume of lateral ventricles in both genotypes. This latter observation appears to depend on age, and not disease state, although ventricular dilations have been reported in very old transgenic P301S rats (Malcolm et al., 2019). The striatal loss, however, appears to be disease relevant and may be a biomarker for bvFTD. It is in line with our behavioural data showing an age-dependent deficit of novel object recognition concomitant to striatal atrophy. While we are the first to reveal an association between novel object recognition deficits and striatal dysfunction observed using MRI, a strong link between dorsal striatum and object discrimination has been reported previously in inactivation studies (Qiao et al., 2017; Korol et al., 2019). While the MRI-recorded striatal atrophy provides a strong anatomical substrate for the observed cognitive deficits in object recognition, it is in contrast with previous MRI studies that reported atrophy of hippocampus and

neocortex in rodent tau models (Wells et al., 2015; Ma et al., 2019; Malcolm et al., 2019; Takeuchi et al., 2020; Ni, 2022). However, it is in agreement with clinical MRI studies of bvFTD patients presenting a strong atrophy of the striatum, that exceeded striatal atrophy in AD patients (Chow et al., 2008; Garibotto et al., 2011; Halabi et al., 2013; Looi and Walterfang, 2013; Bertoux et al., 2015; Macfarlane et al., 2015; Landin-Romero et al., 2017; but see Jakabek et al., 2018) and their presumed functions (Woolley et al., 2013; Sharpe et al., 2019). While limbic volume reductions are also a core feature of bvFTD, there is considerable heterogeneity in patients and a clustering into 4 categories based on MRI volumetric surface renderings has been suggested (Ranasinghe et al., 2016; Whitwell et al., 2009; Vuksanovic et al., 2021). The frontal dominant form of bvFTD is characterised by smaller temporal lobe atrophy; yet reductions in caudate volume are common to all subtypes and was proposed as a diagnostic neuroimaging biomarker for the differential diagnosis of bvFTD (Bertoux et al., 2015; Macfarlane et al., 2015; Landin-Romero et al., 2017). Altogether, this validates our $PLB2_{Tau}$ mouse as a physiologically relevant experimental animal model for bvFTD with truly translational qualities.

The fimbria presented with a substantial age-related lowering of mean diffusivity in $PLB2_{Tau}$ mice. While this may signify an impact on hippocampal function, we did not observe any significant effect on either global hippocampal volume or on MD in different subparts of the hippocampus (dentate gyrus and CA1). A proliferation of glial cells (gliosis) associated with Tau lesions could be responsible for the decrease of diffusivity in the fimbria. The observation of fimbria anomaly per se is interesting in light of the behavioural traits confirmed for aged $PLB2_{Tau}$ mice. Cholinergic input from the basal forebrain medial septum to hippocampus has been suggested as a crucial modulator of arousal/attention (Sarter et al., 2009) and is related to genetic associations with aberrant cortical/hippocampal activity in dementia (Rubido et al., 2024). These anomalies would readily explain the lowering in object exploration in 12 months old $PLB2_{Tau}$ mice and is congruent with the anhedonia phenotype in these mice (Koss et al., 2016).

On the basis of these data, we propose that $PLB2_{Tau}$ mice should serve as a useful model to further elucidating the early development of the pathogenesis of tau-linked bvFTD.

Funding

This work was funded by grants from the CNRS, le Conseil Régional de la Nouvelle Aquitaine and Ecole Pratique des Hautes Etudes (EPHE)

CRediT authorship contribution statement

Jacques Micheau: Writing – review & editing, Writing – original draft, Visualization, Supervision, Resources, Project administration, Methodology, Investigation, Formal analysis, Data curation, Conceptualization. **Gernot Riedel:** Writing – review & editing, Writing – original draft, Visualization, Methodology, Conceptualization. **Bettina Platt:** Writing – review & editing, Writing – original draft, Funding acquisition, Conceptualization. **Michèle Allard:** Writing – review & editing, Project administration. **Anne Marcilhac:** Writing – review & editing, Project administration, Funding acquisition. **Bassem Hiba:** Writing – review & editing, Investigation, Formal analysis. **Elodie Barse:** Writing – review & editing, Investigation. **Gwenaelle Catheline:** Writing – review & editing, Writing – original draft, Formal analysis, Conceptualization.

Declaration of Competing Interest

None declared.

Acknowledgements

The authors acknowledge Dr. Sophie Tronel for graphical display.

Data availability

Data will be made available on request.

References

Ahmed, R.M., Irish, M., van Eersel, J., Ittner, A., Ke, Y.D., Volkerling, A., et al., 2017. Mouse models of frontotemporal dementia: A comparison of phenotypes with clinical symptomatology. Neurosci. Biobehav. Rev. 74, 126–138. https://doi.org/10.1016/j.neubiorev.2017.01.004.

Ameen-Ali, K.E., Sivakumaran, M.H., Eacott, M.J., O'Connor, A.R., Ainge, J.A., Easton, A., 2021. Perirhinal cortex and the recognition of relative familiarity. Neurobiol. Learn. Mem. 182, 107439. https://doi.org/10.1016/j.nlm.2021.107439.

Barendrecht, S., Schreurs, A., Geissler, S., Sabanov, V., Ilse, V., Rieckman, V., et al., 2023. A novel human tau knock-in mouse model reveals interaction of Abeta and human tau under progressing cerebral amyloidosis in 5xFAD mice. Alz. Res. Ther. 15, 16. https://doi.org/10.1186/s13195-022-01144-y.

Bazzari, F.H., Bazzari, A.H., 2022. BACE1 inhibitors for Alzheimer's disease: the past, present and any future? Molecules 27, 8823. https://doi.org/10.3390/molecules27248823.

Bertoux, M., O'Callaghan, C., Flanagan, E., Hodges, J.R., Hornberger, M., 2015. Fronto-striatal atrophy in behavioral variant frontotemporal dementia and Alzheimer's disease. Front. Neurol. 6, 147. https://doi.org/10.3389/fneur.2015.00147.

Brandt, N.J., Wheeler, C., Courtin, S.O., 2023. Navigating disease-modifying treatments for Alzheimer's disease: focusing on medications in phase 3 clinical trials. J. Gerontol. Nurs. 49 (1), 6–10. https://doi.org/10.3928/00989134-20221205-02.

Camargo, L.C., Honold, D., Bauer, R., Shah, N.J., Langen, K.-J., Willbold, D., et al., 2021. Sex-related motor deficits in the Tau-P301L mouse model. Biomedicines 9, 1160. https://doi.org/10.3390/biomedicines9091160.

Carlesimo, G.A., Oscar-Berman, M., 1992. Memory deficits in Alzheimer's patients: a comprehensive review. Neuropsychol. Rev. 3, 119–169 https://doi-org.proxy.insermbiblio.inist.fr/10.1007/BF01108841.

Chao, O.Y., Nikolaus, S., Yang, Y.-M., Huston, J.P., 2022. Neuronal circuitry for recognition memory of object and place in rodent models. Neurosci. Biobehav. Rev. 141, 104855. https://doi.org/10.1016/j.neubiorev.2022.104855.

Chow, T.W., Izenberg, A., Binns, M.A., Freedman, M., Stuss, D.T., Scott, C.J.M., et al., 2008. Magnetic resonance imaging in frontotemporal dementia shows subcortical atrophy. Dement. Geriat. Cogn. Disord. 26, 79–88. https://doi.org/10.1159/000144028.

Cohen, J., 1988. Statistical power analysis for the behavioral sciences. Lawrence Earlbaum Associates, 2nd Ed. Routledge Academic, NJ. https://doi.org/10.1111/1467-8721.ep10768783.

Colgan, N., Siow, B., O'Callaghan, J.M., Harrison, I.F., Wells, J.A., Holmes, H.E., et al., 2016. Application of neurite orientation dispersion and density imaging (NODDI) to a tau pathology model of Alzheimer's disease. NeuroImage 125, 739–744. https://doi.org/10.1016/j.neuroimage.2015.10.043.

Couzin-Frankel, J., 2023. Alzheimer's drug approval gets a mixed reception. Science 379, 6628. https://doi.org/10.1126/science.adg6275.

Couzin-Frankel, J., 2024. New Alzheimer's drug clears FDA advisory vote despite unknowns. Science 384, 6701. https://doi.org/10.1126/science.adr0291.

Couzin-Frankel, J., Piller, C., 2022. Alzheimer's drug stirs excitement-and concerns. Science 378 (6624), 1030–1031. https://doi.org/10.1126/science.adg1899.

Crombé, A., Nicolas, R., Richard, N., Tourdias, T., Hiba, B., 2022. High B-value diffusion tensor imaging for early detection of hippocampal microstructural alteration in a mouse model of multiple sclerosis. Sci. Rep. 12 (1), 12008. https://doi.org/10.1038/s41598-022-15511-0.

Cummings, J., Lee, G., Nahed, P., Kambar, M.E.Z.N., Zhong, K., Fonseca, J., Taghva, K., 2022. Alzheimer's disease drug development pipeline: 2022. Alzheimer'S. Dement 8, e12295. https://doi.org/10.1002/trc2.12295.

Cummings, L.J., Vinters, H.V., Cole, G.M., Khachaturian, Z.S., 1998. Alzheimer's disease: etiologies, pathophysiology, cognitive reserve, and treatment opportunities. Neurology 51, S2–S17. https://doi.org/10.1212/WNL.51.1_Suppl_1.S2.

Davis, K.E., Eacott, M.J., Easton, A., Gigg, J., 2013a. Episodic-like memory is sensitive to both Alzheimer's-like pathological accumulation and normal ageing processes in mice. Behav. Brain Res. 254, 73–82. https://doi.org/10.1016/j.bbr.2013.03.009.

Davis, K.E., Eacott, M.J., Easton, A., Gigg, J., 2013b. Episodic-like memory for What Where-Which occasion is selectively impaired in the 3xTgAD mouse model of Alzheimer's Disease. J. Alzheimers Dis. 33, 681–698. https://doi.org/10.3233/JAD-2012-121543.

Degiorgis, L., Karatas, M., Sourty, M., Faivre, E., Lamy, J., Noblet, V., et al., 2020. Brain network remodelling reflects tau-related pathology prior to memory deficits in Thy-Tau22 mice. Brain 143 (12), 3748–3762. https://doi.org/10.1093/brain/awaa312.

Deiana, S., Platt, B., Riedel, G., 2011. The cholinergic system and spatial learning. Behav. Brain Res. 221 (2), 389–411. https://doi.org/10.1016/j.bbr.2010.11.036.

Dere, E., Zheng-Fischhöfer, Q., Viggiano, D., Gironi Carnevale, U.A., Ruocco, L.A., Zlomuzica, A., 2008. Connexin31.1 deficiency in the mouse impairs object memory and modulates open-field exploration, acetylcholine esterase levels in the striatum, and cAMP response element-binding protein levels in the striatum and piriform cortex. Neuroscience 153 (2), 396–405. https://doi.org/10.1016/j.neuroscience.2008.01.077.

Drever, B.D., Riedel, G., Platt, B., 2011. The cholinergic system and hippocampal plasticity. Behav. Brain Res. 221 (2), 505–514. https://doi.org/10.1016/j.bbr.2010.11.037.

Dyer, O., 2024. Donanemab: FDA experts recommend approval of Alzheimer's drug. BMJ 385, q1327. https://doi.org/10.1136/bmj.q1327.
Eacott, M.J., Norman, G., 2004. Integrated memory for object, place, and context in rats: a possible model of episodic-like memory? J. Neurosci. 24, 1948–1953. https://doi.org/10.1523/JNEUROSCI.2975-03.2004.
Ennaceur, A., Delacour, J., 1988. A new one-trial test for neurobiological studies of memory in rats. 1: Behavioral data. Behav. Brain Res 31 (1), 47–59. https://doi.org/10.1016/0166-4328(88)90157-x.
Espay, A.J., Kepp, K.P., Herrup, K., 2024. Lecanemab and donanemab as therapies for Alzheimer's disease: an illustrated perspective on the data. eNeuro. https://doi.org/10.1523/ENEURO.0319-23.2024.
Fung, C.W., Guo, J., Fu, H., Figueroa, H.Y., Konofagou, E.E., Duff, K.E., 2020. Atrophy associated with tau pathology precedes overt cell death in a mouse model of progressive tauopathy. Sci. Adv. 6, eabc8098 https://doi/10.1126/sciadv.abc8098.
Gamache, J., Benzow, K., Forster, C., Kemper, L., Hlynialuk, C., Furrow, E., et al., 2019. Factors other than hTau overexpression that contribute to tauopathy-like phenotype in rTg4510 mice. Nat. Com. 10, 2479. https://doi.org/10.1038/s41467-019-10428-1.
Garibotto, V., Borroni, B., Agosti, C., Premi, E., Alberici, A., Eickhoff, S.B., et al., 2011. Subcortical and deep cortical atrophy in frontotemporal lobar degeneration. Neurobiol. Aging 32, 875–884. https://doi.org/10.1016/j.neurobiolaging.2009.05.004.
Geiszler, P.C., Barron, M.R., Pardon, M.-C., 2016. Impaired burrowing is the most prominent behavioral deficit of aging HTau mice. Neuroscience 329, 98–111. https://doi.org/10.1016/j.neuroscience.2016.05.004.
Green, C., Sydow, A., Vogel, S., Anglada-Huguet, M., Wiedermann, D., Mandelkow, E., et al., 2019. Functional networks are impaired by elevated tau-protein but reversible in a regulatable Alzheimer's disease mouse model. Mol. Neurodegen. 14, 13. https://doi.org/10.1186/s13024-019-0316-6.
Halabi, C., Halabi, A., Dean, D.L., Wang, P.-N., Boxer, A.L., Trojanowski, J.Q., et al., 2013. Patterns of striatal degeneration in frontotemporal dementia. Alzheimer Dis. Assoc. Disord. 27, 74–83. https://doi.org/10.1097/WAD.0b013e31824a7df4.
Harkotte, M., Contreras, M.P., Inostroza, M., Born, J., 2022. Effects of information load on schema and episodic memory formation. Front. Behav. Neurosci. 16, 923713. https://doi.org/10.3389/fnbeh.2022.923713.
Holmes, H.E., Powell, N.M., Ma, D., Ismail, O., Harrison, I.F., Wells, J.A., et al., 2017. Comparison of *In vivo* and *Ex vivo* MRI for the detection of structural abnormalities in a mouse model of tauopathy. Front. Neuroinform. 11, 20 https://doi/10.3389/fninf.2017.00020.
Hornberger, M., Piguet, O., 2012. Episodic memory in frontotemporal dementia: a critical review. Brain 135, 678–692. https://doi.org/10.1093/brain/aws011.
Hull, C., Dekeryte, R., Buchanan, H., Kamli-Salino, S., Robertson, A., Delibegovic, M., Platt, B., 2020. NLRP3 inflammasome inhibition with MCC950 improves insulin sensitivity and inflammation in a mouse model of frontotemporal dementia. Neuropharmacol 180, 108305. https://doi.org/10.1016/j.neuropharm.2020.108305.
Hull, C., Dekeryte, R., Koss, D., Buchanan, H., Delibegovic, M., Platt, B., 2019. Knock-in of mutated hTAU causes insulin resistance, inflammation and proteostasis disturbance in a mouse model of frontotemporal dementia. Mol. Neurobiol. https://doi.org/10.1007/s12035-019-01722-6.
Huston, J.P., Chao, O.Y., 2023. Probing the nature of episodic memory in rodents. Neurosci. Biobehav. Rev. 144, 104930. https://doi.org/10.1016/j.neubiorev.2022.104930.
Jakabek, D., Power, B.D., Macfarlane, M.D., Walterfang, M., Velakoulis, D., van Western, D., et al., 2018. Regional structural hypo- and hyperconnectivity of frontal–striatal and frontal–thalamic pathways in behavioral variant frontotemporal dementia. Hum. Brain Mapp. 39, 4083–4093. https://doi.org/10.1002/hbm.24233.
Ji, M., Xie, X.X., Liu, D.Q., Yu, X.L., Zhang, Y., Zhang, L.X., et al., 2018. Hepatitis B core VLP-based mis-disordered tau vaccine elicits strong immune response and alleviates cognitive deficits and neuropathology progression in Tau.P301S mouse model of Alzheimer's disease and frontotemporal dementia. Alzheimers Res. Ther. 10 (1), 55. https://doi.org/10.1186/s13195-018-0378-7.
Kinnavane, L., Albasser, M., Aggletown, J.P., 2015. Advances in the behavioural testing and network imaging of rodent recognition memory. Behav. Brain Res. 285, 67–78. https://doi.org/10.1016/j.bbr.2014.07.049.
Kolb, B., Mychasiuk, R., Muhammad, A., Li, Y., Frost D.O., Gibb, R., 2012 Experience and the developing prefrontal cortex. PNAS 109 (supplement_2) 17186-17193. https://doi.org/10.1073/pnas.1121251109.
Korol, D., Gardner, R.S., Tunur, T., Gold, P.E., 2019. Involvement of lactate transport in two object recognition tasks that require either the hippocampus or striatum. Behav. Neurosci. 133 (2), 176–187. https://doi.org/10.1037/bne0000304.
Koss, D.J., Robinson, L., Drever, B.D., Plucińska, K., Stoppelkamp, S., Veselcic, P., et al., 2016. Mutant Tau knock-in mice display frontotemporal dementia relevant behaviour and histopathology. Neurobiol. Dis. 91, 105–123. https://doi.org/10.1016/j.nbd.2016.03.002.
Kubota, T., Kirino, Y., 2021. Age-dependent impairment of memory and neurofibrillary tangle formation and clearance in a mouse model of tauopathy. Brain Res 1765, 147496. https://doi.org/10.1016/j.brainres.2021.147496.
Landin-Romero, R., Kumfor, F., Leyton, C.E., Irish, M., Hodges, J.R., Piguet, O., 2017. Disease-specific patterns of cortical and subcortical degeneration in a longitudinal study of Alzheimer's disease and behavioural-variant frontotemporal dementia. NeuroImage 151, 72–80. https://doi.org/10.1016/j.neuroimage.2016.03.032.
Looi, J.C.L., Walterfang, M., 2013. Striatal morphology as a biomarker in neurodegenerative disease. Mol. Psychiat. 18, 417–424. https://doi.org/10.1038/mp.2012.54.
Ma, D., Holmes, H.E., Cardoso, M.J., Modat, M., Harrison, I.F., Powell, N.M., et al., 2019. Study the longitudinal in vivo and cross-sectional ex vivo brain volume difference for disease progression and treatment effect on mouse model of tauopathy using automated MRI structural parcellation. Front. Neurosci. 13, 11. https://doi.org/10.3389/fnins.2019.00011.
Macchitella, L., Tosi, G., Giaquinto, F., Laia, M., Rizzi, E., Chiarell, Y., et al., 2023. Genuine memory deficits as assessed by the Free and Cued Selective Reminding Test (FCSRT) in the behavioural variant of frontotemporal dementia. A systematic review and meta-analysis study. Neuropsychol. Rev. https://doi.org/10.1007/s11065-023-09613-3.
Macfarlane, M.D., Jakabek, D., Walterfang, M., Vestberg, S., Velakoulis, D., Wilkes, F.A., et al., 2015. Striatal atrophy in the behavioural variant of frontotemporal dementia: correlation with diagnosis, negative symptoms and disease severity. PLoS ONE 10 (6), e0129692. https://doi.org/10.1371/journal.pone.0129692.
Mahase, E., 2023. Alzheimer's disease: FDA approves lecanemab amid cost and safety concerns. BMJ 380, p73. https://doi.org/10.1136/bmj.p73.
Malcolm, J.C., Breuillaud, L., Do Carmo, S., Hall, H., Welikovitch, L.A., Macdonald, J.A., et al., 2019. Neuropathological changes and cognitive deficits in rats transgenic for human mutant tau recapitulate human tauopathy. Neurobiol. Dis. 127, 323–338. https://doi.org/10.1016/j.nbd.2019.03.018.
Marighetto, A., Jaffard, R., Micheau, J., 1994a. Effects of intraseptally injected noradrenergic drugs on hippocampal sodium-dependent-high-affinity-choline-uptake in 'resting' and 'trained' mice. Brain Res 652 (1), 120–128. https://doi.org/10.1016/0006-8993(94)90325-5.
Marighetto, A., Micheau, J., Jaffard, R., 1994b. Effects of intraseptally injected glutamatergic drugs on hippocampal sodium-dependent-high-affinity-choline-uptake in "naïve" and "trained" mice. Pharm. Biochem Behav. 49 (3), 689–699. https://doi.org/10.1016/0091-3057(94)90089-2.
Massalimova, A., Ni, R., Nitsch, R.M., Reisert, M., von Elverfeldt, D., Klohs, J., 2020. Diffusion tensor imaging reveals whole-brain microstructural changes in the P301L mouse model of tauopathy. Neurodegener. Dis. 20 (5-6), 173–184. https://doi.org/10.1159/000515754.
McDade, E., Cummings, J.L., Dhadda, S., Swanson, C.J., Reyderman, L., Kanekiyo, M., et al., 2022. Lecanemab in patients with early Alzheimer's disease: detailed results on biomarker, cognitive, and clinical effects from the randomized and open-label extension of the phase 2 proof-of-concept study. Alzheimer'S. Res. Ther. 14, 191. https://doi.org/10.1186/s13195-022-01124-2.
Mellone, M., Kestoras, D., Andrews, M.R., Dassie, E., Crowther, R.A., Stokin, G.B., et al., 2013. Tau pathology is present in vivo and develops in vitro in sensory neurons from human P301S tau transgenic mice: a system for screening drugs against tauopathies. J. Neurosci. 33 (46), 18175–18189. https://doi.org/10.1523/JNEUROSCI.4933-12.2013.
Miller, B., Llibre-Guerra, J.J., 2019. Frontotemporal dementia. In: Reus, V.I., Lindqvist, D. (Eds.), Handbook of Clinical Neurolgy, 165. Psychopharmacology of Neurologic Disease. https://doi.org/10.1016/B978-0-444-64012-3.00003-4.
Moore, K.B.E., Hung, T.-J., Fortin, J.S., 2023. Hyperphosphorylated tau (p-tau) and drug discovery in the context of Alzheimer's disease and related tauopathies. Drug Discov. Today 28, 103487. https://doi.org/10.1016/j.drudis.2023.103487.
Mullard, A., 2021. Anti-tau antibody failures stack up. Nat. Rev. Drug Discov. 20 (12), 888. https://doi.org/10.1038/d41573-021-00187-4.
Ni, R., 2021. Magnetic resonance imaging in animal models of Alzheimer's disease amyloidosis. Int. J. Mol. Sci. 22, 12768. https://doi.org/10.3390/ijms222312768.
Ni, R., 2022. Magnetic resonance imaging in tauopathy animal models. Front. Aging Neurosci. 13, 791679. https://doi.org/10.3389/fnagi.2021.791679.
Onishi, T., Maeda, R., Terada, M., Sato, S., Fujii, T., Ito, M., et al., 2021. A novel orally active HDAC6 inhibitor T-518 shows a therapeutic potential for Alzheimer's disease and tauopathy in mice. Sci. Rep. 11, 15423. https://doi.org/10.1038/s41598-021-94923-w.
Pandya, S., Nicholls, V.I., Krugliak, A., Davis, S.W., Clarke, A., 2024. Context and semantic object properties interact to support recognition memory. Quat. J. Exp. Psychol. https://doi.org/10.1177/17470218241283028.
Passeri, E., Elkhoury, K., Morsink, M., Broersen, K., Linder, M., Tamayol, A., et al., 2022. Alzheiner's disease: treatment strategies and their limitations. Int. J. Mol. Sci. 23, 13954. https://doi.org/10.3390/ijms232213954.
Patrat, C., Ouimette, J.-F., Rougeulle, C., 2020. X chromosome inactivation in human development. Development 147, dev183095. https://doi.org/10.1242/dev.183095.
Percie du Sert, N., Hurst, V., Ahluwalia, A., Alam, S., Avey, M.T., Baker, M., et al., 2020. The ARRIVE guidelines 2.0: Updated guidelines for reporting animal research. PLoS. Biol. 18 (7), e3000410. https://doi.org/10.1371/journal.pbio.3000410.
Perez-Garcia, G., Bicak, M., Haure-Mirande, J.-V., Perez, G.M., Otero-Pagan, A., Gama Sosa, M.A., et al., 2023. BCI-838, an orally active mGluR2/3 receptor antagonist pro-drug, rescues learning behavior deficits in the PS19 MAPT^{P301S} mouse model of tauopathy. Neurosci. Lett. 797, 137080. https://doi.org/10.1016/j.neulet.2023.137080.
Platt, B., Drever, B., Koss, D., Stoppelkamp, S., Jyoti, A., Plano, A., et al., 2011a. Abnormal cognition, sleep, EEG and brain metabolism in a novel knock-in Alzheimer mouse, PLB1. PLoS One 6 (11), e27068. https://doi.org/10.1371/journal.pone.0027068.
Platt, B., Welch, A., Riedel, G., 2011b. 18FDG-PET imaging, EEG and sleep phenotypes as translational biomarkers for research in Alzheimer's disease. Biochem Soc. Trans. 39 (4), 874–880.
Poos, J.M., Jiskoot, L.C., Papma, J.M., van Swieten, J.C., van den Berg, E., 2018. Meta-analytic review of memory impairment in behavioral variant frontotemporal dementia. J. Int. Neuropsychol. Soc. 24, 593–605. https://doi.org/10.1017/S1355617718000115.

Qiao, Y., Wang, X., Ma, L., Li, S., Liang, J., 2017. Functional inactivation of dorsal medial striatum alters behavioral flexibility and recognition process in mice. Physiol. Behav. 179, 467–477. https://doi.org/10.1016/j.physbeh.2017.07.026.

Ramsden, M., Kotilinek, L., Forster, C., Paulson, J., McGowan, E., SantaCruz, K., et al., 2005. Age-dependent neurofibrillary tangle formation, neuron loss, and memory impairment in a mouse model of human tauopathy (P301L). J. Neurosci. 25 (46), 10637–10647. https://doi.org/10.1523/jneurosci.3279-05.2005.

Ranasinghe, K.G., Rankin, K.P., Pressman, P.S., Perry, D.C., Lobach, I.V., Seeley, W.W., et al., 2016. Distinct subtypes of behavioral variant frontotemporal dementia based on patterns of network degeneration. JAMA Neurol. 73 (9), 1078–1088. https://doi.org/10.1001/jamaneurol.2016.2016.

Rollins, C.P.E., Gallino, D., Kong, V., Ayranci, G., Devenyi, G.A., Germann, J., Chakravarty, M.M., 2019. Contributions of a high-fat diet to Alzheimer's disease-related decline: A longitudinal behavioural and structural neuroimaging study in mouse models. Neuroimage Clin. 21, 101606. https://doi.org/10.1016/j.nicl.2018.11.016.

Rubido, N., Riedel, G., Vuksanovic, V., 2024. Genetic basis of anatomical asymmetry and aberrant dynamic functional networks in Alzheimer's disease. Brain Commun. 6 (1), fcad320. https://doi.org/10.1093/braincomms/fcad320.

Ryan, D., Koss, D., Porcu, E., Woodcock, H., Robinson, L., Platt, B., Riedel, G., 2013. Spatial learning impairments in PLB1Triple knock-in Alzheimer mice are task-specific and age-dependent. Cell Mol. Life Sci. 70 (14), 2603–2619. https://doi.org/10.1007/s00018-013-1314-4.

Sahara, N., Perez, P.D., Lin, W.-L., Dickson, D.W., Ren, Y., Zeng, H., et al., 2014. Age-related decline in white matter integrity in a mouse model of tauopathy: an in vivo diffusion tensor magnetic resonance imaging study, 1364e1374 Neurobiol. Aging 35. https://doi.org/10.1016/j.neurobiolaging.2013.12.009.

SantaCruz, K., Lewis, J., Spires, T., Paulson, J., Kotilinek, L., Ingelsson, M., et al., 2005. Tau suppression in a neurodegenerative mouse model improves memory function. Science 309 (5733), 476–481. https://doi.org/10.1126/science.1113694.

Sarter, M., Parikh, V., Howe, W.M., 2009. Phasic acetylcholine release and the volume transmission hypothesis: time to move on. Nat. Rev. Neurosci. 10 (5), 383–390. https://doi.org/10.1038/nrn2635.

Scullion, S.E., Barker, G.R.I., Warburton, E.C., Randall, A.D., Brown, J.T., 2019. Muscarinic receptor-dependent long term depression in the perirhinal cortex and recognition memory are impaired in the rTg4510 mouse model of tauopathy. Neurochem. Res. 44, 617–626. https://doi.org/10.1007/s11064-018-2487-x.

Sharpe, M.J., Stalnaker, T., Schuck, N.W., Killcross, S., Schoenbaum, G., Niv, Y., 2019. An Integrated model of action selection: distinct modes of cortical control of striatal decision making. Annu. Rev. Psychol. 70, 53–76. https://doi.org/10.1146/annurev-psych-010418-102824.

Sun, X.-Y., Li, L.-J., Dong, Q.-X., Zhu, J., Huang, Y.-R., Hou, S.-J., et al., 2021. Rutin prevents tau pathology and neuroinflammation in a mouse model of Alzheimer's disease. J. Neuroinflamm. 18, 131. https://doi.org/10.1186/s12974-021-02182-3.

Takeuchi, H., Iba, M., Inoue, H., Higuchi, M., Takao, K., Tsukita, K., et al., 2011. P301S mutant human tau transgenic mice manifest early symptoms of human tauopathies with dementia and altered sensorimotor gating. PLoS One 6 (6), e21050. https://doi.org/10.1371/journal.pone.0021050.

Takeuchi, H., Imamura, K., Ji, B., Tsukita, K., Enami, T., Takao, K., et al., 2020. Nasal vaccine delivery attenuates brain pathology and cognitive impairment in tauopathy model mice. Npj Vaccin. 5, 28. https://doi.org/10.1038/s41541-020-0172-y.

Tong, B.C.-K., Huang, A.S., Wu, A.J., Iyaswamy, A., Ho, O.K.-Y., Kong, A.H.-Y., et al., 2022. Tetrandrine ameliorates cognitive deficits and mitigates tau aggregation in cell and animal models of tauopathies. J. Biomed. Sci. 29, 85. https://doi.org/10.1186/s12929-022-00871-6.

Tounekti, S., Troalen, T., Bihan-Poudec, Y., Froesel, M., Lamberton, F., Ozenne, V., et al., 2018. High-resolution 3D diffusion tensor MRI of anesthetized rhesus macaque brain at 3T. Neuroimage 181, 149–161. https://doi.org/10.1016/j.neuroimage.2018.06.045.

Tulloch, J., Netsyk, O., Pickett, E.K., Herrmann, A.G., Jain, P., Stevenson, A.J., et al., 2021. Maintained memory and long-term potentiation in a mouse model of Alzheimer's disease with both amyloid pathology and human tau. Eur. J. Neurosci. 53, 637–648. https://doi.org/10.1111/ejn.14918.

Vuksanović, V., Staff, R.T., Morson, S., Ahearn, T., Bracoud, L., Murray, A.D., 2021. Degeneration of basal and limbic networks is a core feature of behavioural variant frontotemporal dementia. Brain Com. 1–15. https://doi.org/10.1093/braincomms/fcab241.

Wang, C., Chang, Y., Zhu, J., Wu, Y., Jiang, X., Zheng, S., et al., 2023. AdipoRon mitigates tau pathology and restores mitochondrial dynamics via AMPK-related pathway in a mouse model of Alzheimer's disease. Exp. Neurol. 363, 114355. https://doi.org/10.1016/j.expneurol.2023.114355.

Welch, A., Mingarelli, M., Riedel, G., Platt, B., 2013. Mapping Changes in Mouse Brain Metabolism with PET/CT. J. Nucl. Med. 54, 1946–1953.

Wells, J.A., O'Callaghan, J.M., Holmes, H.E., Powell, N.M., Johnson, R.A., Siow, B., et al., 2015. In vivo imaging of tau pathology using multi-parametric quantitative MRI. NeuroImage 111, 369–378. https://doi.org/10.1016/j.neuroimage.2015.02.023.

Werner, J.M., Hover, J., Gillis, J., 2024. Population variability in X-chromosome inactivation across 10 mammalian species. Nat. Comm. 15, 8991. https://doi.org/10.1038/s41467-024-53449-1.

Whitwell, J.L., Przybelski, S.A., Weigand, S.D., Ivnik, R.J., Vemuri, P., Gunter, J.L., et al., 2009. Distinct anatomical subtypes of the behavioural variant of frontotemporal dementia: a cluster analysis study. Brain 132, 2932–2946. https://doi.org/10.1093/brain/awp232.

Wilcock, G.K., Gauthier, S., Frisoni, G.B., Jia, J., Hardlund, J.H., Moebius, H.J., et al., 2018. Potential of low dose Leuco-Methylthioninium Bis(Hydromethanesulphonate) (LMTM) monotherapy for treatment of mild Alzheimer's Disease: cohort analysis as modified primary outcome in a phase III clinical trial. J. Alzheimers Dis. 61 (1), 435–457. https://doi.org/10.3233/JAD-170560.

Wischik, C.M., Bentham, P., Gauthier, S., Miller, S., Kook, K., Schelter, B.O., 2022. Oral Tau aggregation inhibitor for Alzheimer's disease: design, progress and basis for selection of the 16 mg/day dose in a phase 3, randomized, placebo-controlled trial of hydromethylthionine mesylate. J. Prev. Alzheimers Dis. 9 (4), 780–790. https://doi.org/10.14283/jpad.2022.63.

Wong, S., Irish, M., Savage, G., Hodges, J.R., Piguet, O., Hornberger, M., 2018. Strategic value-directed learning and memory in Alzheimer's disease and behavioural-variant frontotemporal dementia. J. Neuropsychol. https://doi.org/10.1111/jnp.12152.

Woolley, D.G., Laeremans, A., Gantois, I., Mantini, D., Vermaercke, B., Op de Beeck, H.P., 2013. Homologous involvement of striatum and prefrontal cortex in rodent and human water maze learning. PNAS 110 (8), 3131–3136. ⟨www.pnas.org/cgi/doi/10.1073/pnas.1217832110⟩.

Yang, S., Cacquevel, M., Saksida, L.M., Bussey, T.J., Schneider, B.L., Aebisher, P., et al., 2015. Perineuronal net digestion with chondroitinase restores memory in mice with tau pathology. Exp. Neurol. 265, 48–58. https://doi.org/10.1016/j.expneurol.2014.11.013.

Yang, S., Hilton, S., Alves, J.N., Saksida, L.M., Bussey, T.J., Matthews, R.T., et al., 2017. Antibody recognizing 4-sulfated chondroitin sulfate proteoglycans restores memory in tauopathy-induced neurodegeneration. Neurobiol. Aging 59, 197–209. https://doi.org/10.1016/j.neurobiolaging.2017.08.002.

Yokoyama, M., Kobayashi, H., Tatsumi, L., Tomita, T., 2022. Mouse models of Alzheimer's disease. Front. Mol. Neurosci. 15, 912995. https://doi.org/10.3389/fnmol.2022.912995.